NONLINEAR STATE ESTIMATION OF VAN DER POL OSCILLATOR USING PARTICLE FILTER WITH UNSCENTED KALMAN FILTER AS PROPOSAL

D. JAYAPRASANTH, S. KANTHALAKSHMI
Department of Instrumentation and Control systems Engineering, PSG College of Technology
Tamil Nadu, India
Email: djp@ice.psgtech.ac.in, skl@ice.psgtech.ac.in

Abstract: *State estimation is a major problem in industrial systems. The accurate estimation of states leads to effective monitoring of system, fault diagnosis and good control performance. The particle filter is potentially suited for better estimation of highly nonlinear and non-Gaussian system. The selection of a suitable importance proposal density is a crucial step in the design of particle filter. The unscented Kalman filter (UKF) provides better state estimates for a nonlinear system than the well known extended Kalman filter (EKF). The particle filter using an UKF to generate proposal density is referred as unscented particle filter (UPF). The potential advantage of UPF is that the UKF allows the particle filter to incorporate the latest measurements in to a prior updating routine. This paper proposes an application of UPF in the field of electrical engineering, with special emphasis on highly nonlinear Van der Pol oscillator (VPO). Simulation tests were carried out on VPO system to assess the state estimation performance of the sampling importance resampling particle filter (SIR-PF) and UPF under various conditions such as initial state estimate mismatch, large measurement noise and model error. The results indicate that the UPF is highly robust and provides accurate estimation of states than the SIR-PF.*

Key words: *Van der Pol oscillator, state estimation, particle filter, importance proposal density, unscented particle filter.*

1. Introduction

It is well known that the oscillator plays a vital role in the development of industrial electronics. An oscillator considered in this work is a nonlinear Van der Pol oscillator (VPO). The VPO is the keystone for studying systems with limit cycle oscillations due to its unique nature. It is also a widely used example in the literature because of its interesting behavior [1-3]. It can exhibit both stable limit cycle and unstable limit cycle depending on the direction of time [4]. In the recent years, many research works have been carried out related to the control of chaotic systems [5-8]. As the reported work on the VPO is extensive in the literature, only a very small part of it deals with the probabilistic aspects of this oscillator, i.e., the state estimation performance when the VPO is subjected to stochastic noises.

Over the last few decades, state estimation has been largely applied to many engineering problems for estimating the states of the dynamical system using a sequence of noisy measurements. Currently, the state estimation is becoming an important aspect in the field of electrical engineering also for fault diagnosis, control and performance monitoring applications [9-11]. The Kalman filter (KF) is an optimal state estimator for linear dynamical systems subject to Gaussian noise [12,13]. Most of the practical systems by nature exhibit some degree of nonlinearity. One of the generalizations of the KF is the extended Kalman filter (EKF) which uses nonlinear models directly in order to estimate the states of a nonlinear system [14]. It adopts first order Taylor series expansion to provide a local linearization of the system around the operating point at each time instant [9]. Thus the EKF neither has a proof of its convergence nor a proof that the resulting estimation satisfies optimality criteria [10]. The unscented Kalman filter (UKF) addresses the approximation issues of the EKF by deterministically choosing a minimal set of sample points and propagating it through the true nonlinear system in a simple and most effective way without making any linear approximations. Hence, the UKF can provide better state estimates than the EKF [15,16]. Like EKF, the UKF also assumes Gaussian posterior density but both these filters do not address non-Gaussian distributions.

In order to overcome the limitations of the Kalman filter- based estimators, the particle filter which can perform equally well for Gaussian and non-Gaussian distributions has been proposed for state estimation of a nonlinear system [17]. The importance proposal density is a vital design choice of the particle filter that will significantly affect its performance. In the sequential importance resampling particle filter (SIR-PF), the transition prior is chosen as proposal density which does not make use of current measurement to propose new particles. So due to such weaker assumptions, the SIR-PF may become inefficient [18]. The UKF algorithm which does not involve analytical linearization and computation of Jacobians is used as proposal for the particle filter in this work to develop an efficient particle filtering algorithm known as unscented particle filter (UPF) [19]. Unlike SIR-PF, the UPF makes use of the measurement model and the information present in the current measurement to propose new particles [20-22].

Many variants of particle filters have been

developed in the recent years and applied to various fields of engineering [23-25]. There has, however, been a limited application of particle filters in the field of electrical engineering [24]. Kalman filter based estimators such as EKF and UKF for estimating the states of highly nonlinear Van der Pol oscillator (VPO) was reported in [2,26]. Sajeeb et al. [3] provides improvement over earlier works by using the particle filter for VPO. But in [3], a semi-analytical particle filter used for the state estimation problem of nonlinear VPO involves the complex analytical approximation approach in the particle filtering algorithm which is cumbersome. The work carried out in this paper addresses the above issue for the nonlinear oscillator by using the concept of (deterministic) sample statistics in the particle filter approach which is free from analytical calculations. As the deterministic sampling technique is used in the particle filter framework, the chances of error being introduced in the design of such filter for VPO can be very minimum. Therefore, this paper focuses on using the UPF for nonlinear state estimation of VPO and its estimation performance is evaluated in comparison with the sampling importance resampling particle filter (SIR-PF). The robustness of the UPF is also tested under different conditions such as initial state mismatch, large measurement noise and model error.

2. Van der Pol Oscillator

The study of nonlinear oscillators has been important in the development of the theory of nonlinear dynamical systems [1]. Unlike linear oscillator, the nonlinear oscillator is structurally stable and the amplitude of oscillation is independent of initial conditions. Earlier, Van der Pol investigated electrical circuits employing vacuum tubes and found that they have stable oscillations and also constructed a circuit model of the human heart to study the range of stability of heart dynamics, which later came to be known as Van der Pol Oscillator [4]. The Van der Pol oscillator (VPO), an oscillator with nonlinear damping is a highly nonlinear system [27].

In the harmonic oscillator, there is a continuum of periodic orbits but in the case of VPO, there is only one isolated periodic orbit which is called as limit cycle. A limit cycle is a closed trajectory in phase plane having the property that at least one other trajectory spirals in to it either as time approaches infinity or as time approaches negative infinity. The limit cycle is used to describe the perfect behavior of the VPO. If all the neighboring trajectories approach the limit cycle as time approaches infinity (forward time), it is called as stable limit cycle. Instead, if all the neighboring trajectories approach the limit cycle as time tends to negative infinity (reverse time) then it is called as unstable limit cycle [2].

2.1 Mathematical model of Van der Pol oscillator

The VPO for analyzing the nonlinear oscillations can be regarded as a RLC circuit with a negative-nonlinear resistor which has the ability to pump energy in to the system or a parallel RLC circuit linked to a triode valve as the amplifier, with the anode current in the triode being a nonlinear function of the lumped voltage [1,27]. The dynamics of VPO in electrical circuits is governed by a second order nonlinear differential equation as

$$\ddot{x} + \mu(x^2 - 1)\dot{x} + x = 0 \tag{1}$$

where x is the position coordinate which is a function of time and μ is a control parameter that reflects the degree of nonlinearity of the VPO system. For example, the system nonlinearity increases for increase in the value of μ. The Van der Pol equation in (1) has become a staple model for most of the oscillatory processes in industries [26]. It can describe self-sustained oscillations in the form of limit cycles. The system will enter in to a stable limit cycle for $\mu > 0$ and an unstable limit cycle for $\mu < 0$. This differential equation possesses a periodic solution that attracts other solution except the trivial one at the unique equilibrium point $x = \dot{x} = 0$.

The state equations of the VPO, with $x_1 = x$, $x_2 = \dot{x}$ in (1) are as follows:

$$\dot{x}_1 = x_2,$$

$$\dot{x}_2 = -x_1 - \mu(x_1^2 - 1)x_2 \tag{2}$$

The measurement equation is given as

$$y = [x_1 \quad x_2]^{\mathrm{T}} \tag{3}$$

As the Van der Pol equation is commonly used to model the processes involving nonlinear oscillations, the studies on state estimation of VPO is generally carried out in the literature by considering its states as x_1, x_2 and the same is followed in this work [2,3,26]. A phase portrait is usually constructed to study the nature of the VPO system. This phase portrait depends on the selection of the value of μ. The importance of the control parameter μ in the VPO is further provided by considering the three cases as follows:

- When $\mu = 0$, there is no damping function and the system functions as the simple harmonic oscillator.
- When $\mu > 0$, the system will enter a stable limit cycle where energy continues to be conserved.
- When $\mu < 0$, the system will be damped and exhibit an unstable limit cycle.

3. Particle Filter

The particle filter based on sequential Monte Carlo (SMC) method generates a large number of samples (particles) to approximate the posterior probability of the states [17]. If the state and measurement functions are nonlinear, and the process and measurement noises are non-Gaussian then the particle filter has the ability to give superior performance than the EKF and UKF [24]. For nonlinear systems, even when the process and measurement noise are initially assumed to be Gaussian, the distribution becomes non-Gaussian after they pass through the nonlinear dynamic system [21].

The basic framework for the particle filter involves the state estimation of a stochastic nonlinear dynamic system given by (4) and (5),

$$x_k = f(x_{k-1}, u_{k-1}, v_{k-1}) \tag{4}$$

$$y_k = g(x_k, n_k) \tag{5}$$

where k is the time index, x_k represents state of the system, u_k signifies system input, y_k represents noisy measurement of the system, v_k and n_k are considered as process noise with covariance Q and measurement noise with covariance R respectively. It is assumed that the stochastic noises v_k and n_k are uncorrelated. The function $f(.)$ and $g(.)$ represents the nonlinear state and measurement functions respectively.

The main idea of particle filter is to approximate the required posterior probability density $p(x_k \mid y_{1:k})$ of the state x_k by a large number of random particles $\{x_k^i, i = 1,..., N_p\}$ with associated weights $\{w_k^i, i = 1,..., N_p\}$ and to compute the state estimates based on these particles and weights [28]. N_p refers to the number of particles. The posterior probability density can then be approximated by the following empirical density function as

$$p(x_k \mid y_{1:k}) \approx \sum_{i=1}^{N_p} w_k^i \delta(x_k - x_k^i) \tag{6}$$

where $\delta(x)$ is the Dirac delta function which is equal to unity if $x = 0$; otherwise it is equal to zero. Hence, the vital step is to draw random particles from the posterior density $p(x_k \mid y_{1:k})$ but since $p(x_k \mid y_{1:k})$ is not of the conventional form such as Gaussian pdf, it becomes impossible to draw particles. Therefore, the particle filter relies on importance sampling method and uses importance proposal density $\pi(x_k \mid y_{1:k})$ and drawing particles from the proposal density would be equivalent to drawing particles from the posterior density [18]. So the selection of the proposal density $\pi(x_k \mid y_{1:k})$ is one of the most critical design issue in the particle filter algorithm because the incorrectly chosen proposal density may result in poor filter estimation response [29].

The SIR-PF uses the prior density (transition prior) $p(x_k^i \mid x_{k-1}^i)$ as proposal density and employs the resampling technique for eliminating the particles with smaller weight and creating copies of particles with higher weight, thereby, avoiding the degeneracy phenomenon [28]. The proposal density for such variant of particle filter is defined as

$$\pi(x_k^i \mid x_{k-1}^i, y_k) = p(x_k^i \mid x_{k-1}^i) \tag{7}$$

The importance weights w_k^i for this choice of proposal is obtained as

$$w_k^i = p(y_k \mid x_k^i), \tag{8}$$

and then the weights obtained from (8) are normalized to $\tilde{w}_k^i$ before the resampling stage.

Thus in the SIR-PF, a new particle set is regenerated by sampling with replacement from the original set $\{x_k^i, i = 1,..., N_p\}$ with probability $p(x_k^j = x_k^i) = \tilde{w}_k^i$. The index j indicates the particle index after resampling [25]. Therefore, the resulting particles are considered as independent and identically distributed (i.i.d.) particles from an approximated discrete density function given in (6) and its corresponding normalized importance weights are assumed to be uniform which can be expressed as

$$\tilde{w}_k^i = \frac{1}{N_p} \tag{9}$$

Therefore, the estimated state $\hat{x}_k$ using the SIR-PF is calculated as

$$\hat{x}_k = \frac{1}{N_p} \sum_{j=1}^{N_p} x_k^j \tag{10}$$

As the proposal density for the SIR-PF is independent of the current measurement y_k, the states are estimated without any knowledge of the measurements. Hence, this filter becomes sensitive to outliers and can be inefficient because the assumptions made in this filter are very weak. Also the resampling step applied recursively at every iteration in the SIR filter can result in rapid loss of diversity in particles. An alternative approach is to use a special variant of the particle filter which involves the proposal density dependant on the most recent measurements [28]. Filters with such an importance density are generally

known as local linearization particle filters. It involves the Kalman filter based estimators such as EKF or UKF as proposal [29]. The particle filter using EKF as proposal is referred as extended Kalman particle filter (EKPF). But the EKF may perform poorly for highly nonlinear systems [30,31]. It can also introduce an instability problem due to analytic local linearization approach which involves the computation of Jacobians. Therefore, the particle filter with proposal density generated by the EKF is not always reliable [19].

4. Unscented Particle Filter

A more reliable proposal density for the particle filter was proposed in [19]. The UKF used as proposal with in a particle filter framework is called the unscented particle filter (UPF). The UPF has the ability to solve the state estimation problem in a stochastic highly nonlinear system. The UPF proves to be more robust in estimating the states of a system under high plant-model mismatch [21].

The UKF uses the unscented transformation (UT) method to pick a minimal set of sample points called as sigma points around the mean. The UT forms the algorithmic core of the UKF and it is based on the principle that it is easier to approximate a Gaussian distribution than an arbitrary nonlinear function [15]. The UKF also referred as the so-called derivative free Kalman filter is accurate up to second order for any nonlinearity in estimating the mean and covariance of the states [16]. Therefore, the UKF has the potential of generating proposal density for the particle filter that matches the true posterior density more closely and also has the capability to control the approximation errors in the higher order moments of the proposal density, allowing for heavier tailed distributions than the EKF [19,21].

The idea of UPF is to use a separate UKF to generate a Gaussian proposal density and allowing each particle to propagate through it, i.e.,

$$\pi(x_k^i \mid x_{k-1}^i, y_k) = \mathcal{N}(x_k^i; \hat{x}_k^i, P_k^i) \tag{11}$$

where $\hat{x}_k^i$ and P_k^i are the estimate of the mean and covariance of a particle respectively. The symbol $\mathcal{N}$ represents that the UKF assumes Gaussian distribution. In summary, the UPF algorithm for the time index k is as follows [29]:

a) For $i = 1 : N_p$
   - Run UKF Algorithm (for each particle i)
     $[\hat{x}_k^i, P_k^i] = \text{UKF}[x_{k-1}^i, P_{k-1}^i, y_k]$
   - Draw a sample from the proposal density, i.e. $x_k^i \sim \mathcal{N}(x_k^i; \hat{x}_k^i, P_k^i)$
   - Calculate importance weight, $w_k^i = \dfrac{p(y_k \mid x_k^i)\, p(x_k^i \mid x_{k-1}^i)}{\pi(x_k^i \mid x_{k-1}^i, y_k)}$

   End
b) Normalize the importance weights
c) Resample to get an updated particle set $\{x_k^j, i^j\}_{j=1}^{N_p}$, where j refers to the index of the particle after resampling.
d) For $i = 1 : N_p$
   - Assign Covariance: $P_k^j = P_k^{i^j}$

   End

The output of the UPF algorithm is the mean $\hat{x}_k$ of the updated particle set which is computed as in (10).

5. Simulation Results and Analysis

Simulations of VPO system and its state estimation with SIR-PF and UPF have been carried out using MATLAB program in an open loop condition. It should also be noted that in order to know effectively the estimation performance of the filters, performance comparison of the SIR-PF and UPF is realized in a simulation environment by taking into consideration their estimation errors under the same test conditions. For example, the initial state estimate, initial state covariance, and process and measurement noise covariance are chosen to be the same for both the particle filters considered for estimation in this work. Unlike SIR filter, the UPF propagates the particles towards the likelihood function as a result of which very minimum number of particles can be considered in order to achieve better estimation performance [29]. Hence in this simulation study, the particle count N_p is chosen as 150 for SIR-PF and only 15 for UPF which is about ten times lesser than the other. Simulations have been carried out for 250 sampling instances with a sampling interval of 0.1 sec.

The root mean square error (RMSE) gives the measure of the estimation performance of the filters because it facilitates quantitative comparison. The RMSE values for a Monte Carlo run is defined as

$$\text{RMSE} = \left(\frac{1}{t} \sum_{k=1}^{t} \left(x_k - \hat{x}_k \right)^2 \right)^{1/2} \tag{12}$$

where x_k and $\hat{x}_k$ are true and estimated state at the time step k respectively and t indicates the total number of time steps. To further investigate the robustness of the UPF over SIR-PF to the random perturbations, 100 Monte Carlo simulations are performed with different process and measurement noise realizations of same variance. Thus an average value of the calculated

RMSE for each noise realization is taken as the performance index for filters.

5.1 Design of particle filters for VPO system

This section focuses on the equations and the parameters considered for the process and filters used in this work. The true states of the VPO system is computed at each sampling instant k by solving the state equation given in (13) using the ode solver function in MATLAB.

$$\begin{bmatrix} \dot{x}_1 \\ \dot{x}_2 \end{bmatrix} = \begin{bmatrix} x_2 \\ -x_1 - \mu(x_1^2 - 1)x_2 \end{bmatrix} \tag{13}$$

As the VPO in this work is considered to be a stochastic nonlinear dynamic system, the random noises are assumed to be present in both the state and measurement equations of the true (actual) system. So the true state x_k and the actual measurement y_k is represented as

$$x_k = \begin{bmatrix} x_1 \\ x_2 \end{bmatrix} + v_k$$

$$y_k = x_k + n_k \tag{14}$$

where the states x_1 and x_2 in (14) indicates the states obtained at the instant $k-1$. v_k is the zero mean white process noise with covariance Q and n_k is the zero mean white measurement noise with covariance R. Both these noises are assumed to be independent of past and current state. The randn function in MATLAB is used to generate random values of order 2x1 for the process noise and measurement noise. The values of the initial state $x_0 = \begin{bmatrix} x_1 & x_2 \end{bmatrix}^{\mathrm{T}}$ and control parameter μ considered for each case of VPO is highlighted in the section 5.2 and section 5.3.

The design of UKF forms the core in the development of the UPF for VPO system which is discussed here. Initially, random number of particles $\{x_k^i, i = 1, ..., N_p\}$ are generated and then each particle is made to propagate through the UKF algorithm. As a result, the mean $\hat{x}_k^i$ and covariance P_k^i of the particle x_k^i is obtained from the UKF which is the proposal density in this particle filtering design [29]. The UKF algorithm for the time index k and its design for VPO are as follows:

Calculation of sigma points:

The estimated state $\hat{x}_{k-1}$ at the previous time index is augmented with the mean of the process noise v_k and measurement noise n_k as

$$x_{k-1}^a = \begin{bmatrix} \hat{x}_{k-1}^{\mathrm{T}} & E[v_k^{\mathrm{T}}] & E[n_k^{\mathrm{T}}] \end{bmatrix}^{\mathrm{T}} \tag{15}$$

In the unscented particle filtering framework, the mean of the i^{th} particle at the previous instant, $\hat{x}_{k-1}^{\mathrm{i}}$ is augmented with the mean of the noises and so the above equation is modified as

$$x_{k-1}^a = \begin{bmatrix} \left(\hat{x}_{k-1}^{\mathrm{i}}\right)^{\mathrm{T}} & 0 & 0 & 0 & 0 \end{bmatrix}^{\mathrm{T}} \tag{16}$$

where the augmented term x_{k-1}^a is of the order 6x1 in this work. The initial state estimate $\hat{x}_0$ chosen for each case of VPO is shown in the sections below.

Similarly, the covariance matrix P_{k-1}^i of the i^{th} particle is also augmented with the process noise covariance Q and measurement noise covariance R as

$$P_{k-1}^a = \begin{bmatrix} P_{k-1}^i & 0 & 0 \\ 0 & Q & 0 \\ 0 & 0 & R \end{bmatrix} \tag{17}$$

The values of covariance matrices P, Q and R of the order 2x2 are shown in the following sections from which the augmented covariance matrix P^a of the order 6x6 is calculated.

Calculate $2L+1$ sigma points from the augmented state and covariance to form the sigma point matrix as

$$\mathcal{X}_{k-1}^a = \begin{bmatrix} x_{k-1}^a & x_{k-1}^a \pm \left(\sqrt{(L+\lambda)P_{k-1}^a}\right) \end{bmatrix} \tag{18}$$

where $L = \left(L_x + L_v + L_n\right)$ is the augmented state dimension and $\lambda = \alpha^2(L+\kappa) - L$ is a scaling parameter. α and κ are tuning parameters. Choose $\kappa \geq 0$ to guarantee positive semi-definiteness of the covariance matrix. α is a factor determining the spread of sigma points around the mean. Choose $0 \leq \alpha \leq 1$ and it should ideally be a small number to minimize higher order effects when the nonlinearities are strong.

This filter design for the 2-dimensional VPO system considers the augmented state dimension $L = 6$ from which 13 sigma points are calculated to form the sigma point matrix as in (18). The filter tuning parameters are chosen as $\alpha = 0.01$ and $\kappa = 0$ from which the scaling parameter λ is computed.

The sigma point matrix calculated in (18) can also be represented as

$$\mathcal{X}_{k-1}^{a} = \begin{bmatrix} \mathcal{X}_{k-1}^{x} \\ \mathcal{X}_{k-1}^{v} \\ \mathcal{X}_{k-1}^{n} \end{bmatrix} \tag{19}$$

where the superscripts x, v and n refer to a partition conformal to the dimension of the state, process noise and measurement noise respectively.

Time update equations:

Transform the sigma points through the nonlinear system function,

$$\mathcal{X}_{k|k-1}^{x} = f(\mathcal{X}_{k-1}^{x}, \mathcal{X}_{k-1}^{v}) \tag{20}$$

where the above nonlinear function f is the state function of nonlinear VPO system given in (13).

Calculate the prior estimate of the state and covariance as

$$\hat{x}_{k|k-1} = \sum_{i=0}^{2L} W_{(m)}^{i} \mathcal{X}_{i,k|k-1} \tag{21}$$

$$P_{k|k-1} = \sum_{i=0}^{2L} W_{(c)}^{i} [\mathcal{X}_{i,k|k-1} - \hat{x}_{k|k-1}][\mathcal{X}_{i,k|k-1} - \hat{x}_{k|k-1}]^{\mathrm{T}} \tag{22}$$

The weights $W_{(m)}^{i}$ and $W_{(c)}^{i}$ are defined as

$$W_{(m)}^{0} = \frac{\lambda}{L+\lambda}, \quad i = 0$$

$$W_{(c)}^{0} = \frac{\lambda}{L+\lambda} + (1 - \alpha^2 + \beta), \quad i = 0$$

$$W_{(m)}^{i} = W_{(c)}^{i} = \frac{1}{2(L+\lambda)}, \quad i = 1,..,2L \tag{23}$$

Choose the parameter $\beta \geq 0$ which is a non-negative weighting term. The parameter β can be used to control the error in the kurtosis (higher order moments) which affects the heaviness of the tails of the posterior distribution. The value of $\beta = 1$ is chosen in this design. Then the selected filter tuning parameters are substituted in (23) to evaluate the weights $W_{(m)}^{i}$ and $W_{(c)}^{i}$ for the mean and covariance respectively.

Measurement update equations:

Transform the sigma points through the measurement function,

$$\mathcal{Y}_{k} = g(\mathcal{X}_{k|k-1}^{x}, \mathcal{X}_{k-1}^{n}) \tag{24}$$

where the above function g is the measurement function of VPO system which is considered to be linear in this work.

Calculate the predicted measurement and its covariance as

$$\hat{y}_{k} = \sum_{i=0}^{2L} W_{(m)}^{i} \mathcal{Y}_{i,k} \tag{25}$$

$$P_{y_k y_k} = \sum_{i=0}^{2L} W_{(c)}^{i} [\mathcal{Y}_{i,k} - \hat{y}_{k}][\mathcal{Y}_{i,k} - \hat{y}_{k}]^{\mathrm{T}} \tag{26}$$

The state-measurement cross covariance matrix is calculated as

$$P_{x_k y_k} = \sum_{i=0}^{2L} W_{(c)}^{i} [\mathcal{X}_{i,k|k-1} - \hat{x}_{k|k-1}][\mathcal{Y}_{i,k} - \hat{y}_{k}]^{\mathrm{T}} \tag{27}$$

The Kalman gain is given as

$$K_{k} = P_{x_k y_k} P_{y_k y_k}^{-1} \tag{28}$$

Therefore, the posterior estimates of the state and covariance is computed as

$$\hat{x}_{k} = \hat{x}_{k|k-1} + K_{k}(y_{k} - \hat{y}_{k}) \tag{29}$$

$$P_{k} = P_{k|k-1} - K_{k} P_{y_k y_k} K_{k}^{\mathrm{T}} \tag{30}$$

Hence, the mean $\hat{x}_{k}^{i}$ and covariance P_{k}^{i} of the particle x_{k}^{i} is calculated using UKF algorithm from (29) and (30) respectively. In the same manner, $\hat{x}_{k}$ and P_{k} are obtained for all the particles. Then the importance weight w_{k} which depends on the likelihood function $p(y_{k} \mid x_{k})$ is calculated for each particle. The likelihood function considered in this design is as follows:

$$p(y_{k} \mid x_{k}^{i}) = \frac{1}{\sqrt{(2\pi)^{2}\left[\det(R)\right]}} \exp\left\{-\frac{1}{2} r_{k}^{(i)\mathrm{T}} R^{-1} r_{k}^{(i)}\right\} \tag{31}$$

where $r_{k}^{(i)}$ is the prediction error based on the i^{th} particle which corresponds to the difference between the actual measurement y_{k} and predicted measurement $\hat{y}_{k}$ of the VPO system with *2*-dimensional state vector and R is the measurement noise covariance.

The importance weight w_{k}^{i} is then normalized as

$$w_k^i = \frac{w_k^i}{\sum_{i=1}^{N_p} w_k^i} \tag{32}$$

The resampling technique is next carried out to select only the particles and its associated covariance with higher importance weight. Finally, average of these updated particles from this UPF algorithm is taken to obtain the state estimate of the VPO system at the instant k. The updated particles and its covariance matrices are used for the next sampling instant and the same procedure is recursively carried out for all the sampling instants.

5.2 State estimation of VPO under stable limit cycle using particle filters

In this section, the state estimates of a VPO system exhibiting stable limit cycle using the SIR-PF and UPF are compared and the filter responses are analysed under different conditions.

The stable limit cycle of the VPO system has the property that all trajectories in the vicinity of the limit cycle ultimately tend towards it as $t \to \infty$. In the case of stable limit cycle, any non-zero initial state converges to a stable limit cycle. The estimation performance of the UPF and SIR-PF are analysed below for different cases.

Table 1
State estimation performance of filter under different conditions for VPO system exhibiting stable limit cycle

Conditions	Average RMSE			
	SIR-PF Estimates		UPF Estimates	
	$\hat{x}_1$	$\hat{x}_2$	$\hat{x}_1$	$\hat{x}_2$
Normal system operating conditions	0.3407	0.3935	0.0453	0.0411
Initial state mismatch and model error	0.5646	0.5296	0.0499	0.0489
Initial state mismatch and large measurement noise	1.0491	1.0977	0.2994	0.3067

Case 1: Normal system operating conditions

In the first case, it is assumed that the states of the VPO system with stable limit cycle are estimated under the normal operating conditions in the absence of initial state and model parameter mismatch. The value of the control parameter μ is chosen as 0.4. The initial state (x_0) and the initial state estimate $(\hat{x}_0)$ are chosen as $\begin{bmatrix}1.2 & 0\end{bmatrix}^{\mathrm{T}}$. The initial state covariance (P), process noise covariance (Q) and measurement noise covariance (R) are chosen as

$$P_0 = 10^{-2}\begin{bmatrix}1 & 0\\ 0 & 1\end{bmatrix},\quad Q = (0.05)^2\begin{bmatrix}1 & 0\\ 0 & 1\end{bmatrix} \text{ and}$$

$$R = (0.05)^2\begin{bmatrix}1 & 0\\ 0 & 1\end{bmatrix} \tag{33}$$

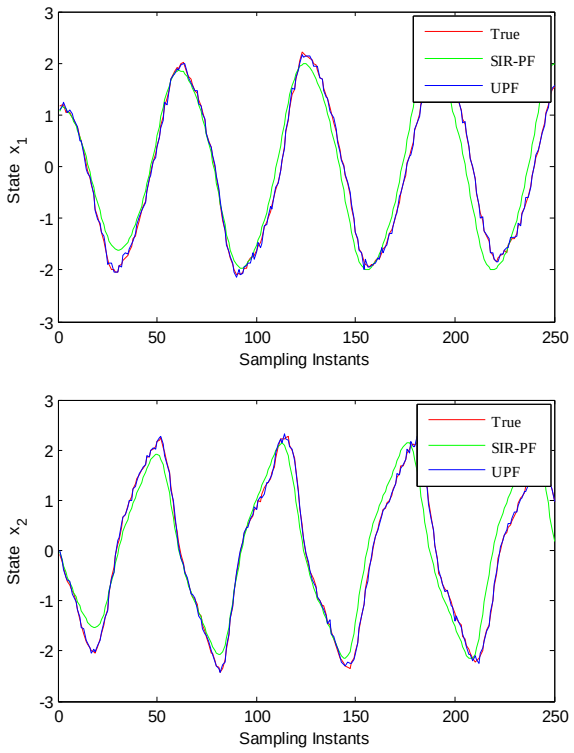

Fig. 1. Evolution of true and estimated states of VPO in forward time using SIR-PF and UPF under normal operating conditions.

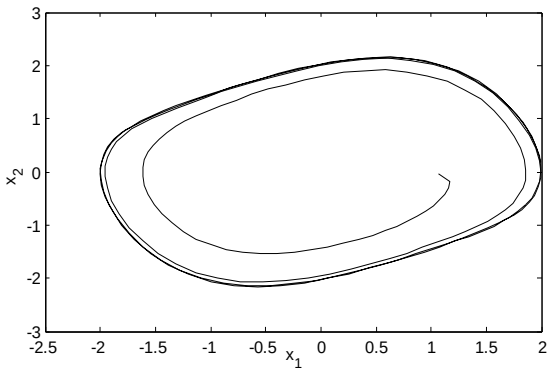

Fig. 2. Phase portrait of SIR-PF estimates under normal operating conditions for VPO exhibiting stable limit cycle.

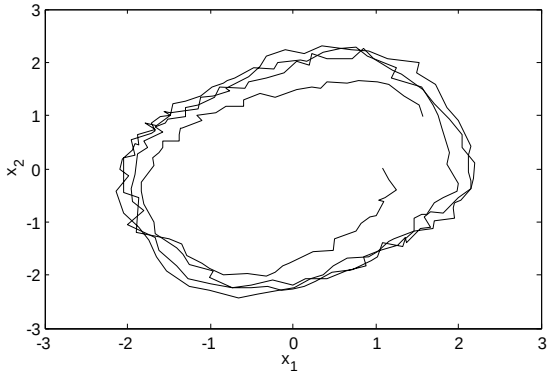

Fig. 3. Phase portrait of UPF estimates under normal operating conditions for VPO exhibiting stable limit cycle.

The true and estimated states using the UPF and SIR-PF are shown in Fig. 1. The UPF estimates tracks closely the true state trajectory as compared to that of SIR-PF. The reason is that the prior density considered as proposal density in the SIR-PF does not allow the particles in the prior to move to the regions of high likelihood.The phase portrait of SIR-PF and UPF estimates representing the closed trajectory of the VPO system in the phase plane are shown in Figs. 2 and 3 respectively. The phase portraits of the UPF depicts that this filter response very closely follows the trajectory of the true system subjected to noise. The average RMSE values of both the filter estimates under normal operating conditions are listed in the first row of Table 1.

Case 2: Initial state and model parameter mismatch

The second case is considered to evaluate the robustness of the UPF over SIR-PF under the presence of model error and initial state estimate mismatch. In the true system and the state estimator model, the value of μ is chosen as 0.4 and 0.6 respectively to introduce model error. The initial state is chosen as $x_0 = \begin{bmatrix} 1.2 & 0 \end{bmatrix}^{\mathrm{T}}$. The initial state estimate $(\hat{x}_0)$, initial state covariance (P), process noise covariance (Q) and measurement noise covariance (R) are chosen as

$\hat{x}_0 = \begin{bmatrix} 0 & 3 \end{bmatrix}^{\mathrm{T}}$,

$P_0 = \begin{bmatrix} 2 & 0 \\ 0 & 2 \end{bmatrix}$, $Q = (0.05)^2 \begin{bmatrix} 1 & 0 \\ 0 & 1 \end{bmatrix}$ and

$$R = (0.05)^2 \begin{bmatrix} 1 & 0 \\ 0 & 1 \end{bmatrix} \tag{34}$$

The choice of P_0 is reasonable here as the initial state estimate is far from the true initial state.

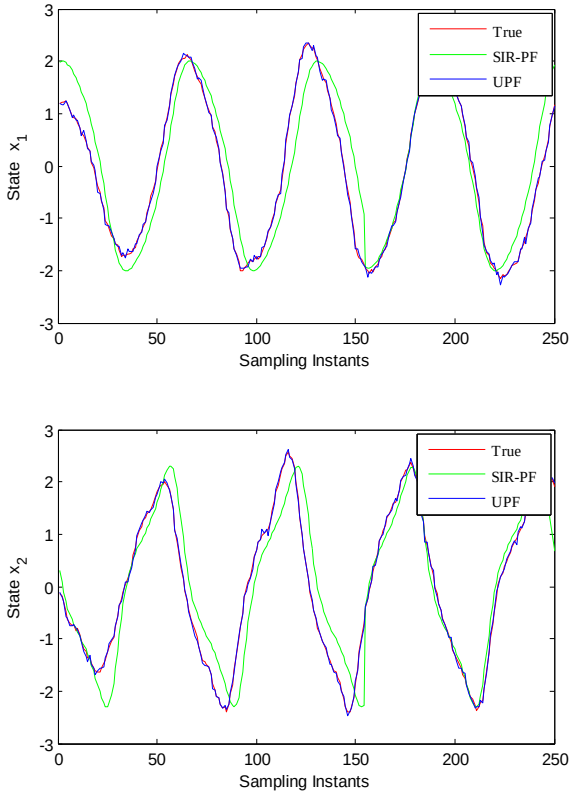

Fig. 4. Evolution of true and estimated states of VPO in forward time using SIR-PF and UPF with large initial state mismatch and model error.

It is observed from Fig. 4 that when there is a significant model error and large initial state mismatch, the UPF is more robust and thereby, giving significantly better estimation results but the SIR-PF estimates are not able to converge to the true states. The phase portrait of SIR-PF and UPF estimates in the presence of initial state mismatch and model error are shown in Figs. 5 and 6 respectively. The average RMSE values calculated for this case are listed in the second row of Table 1.

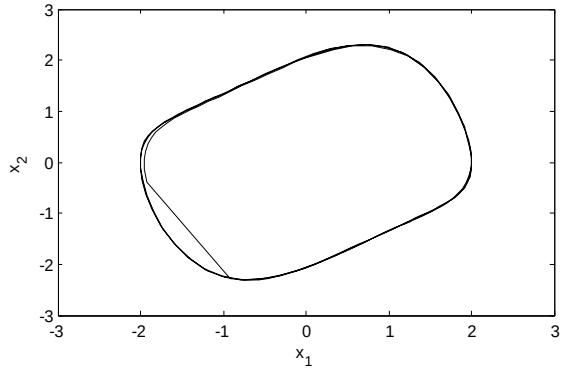

Fig. 5. Phase portrait of SIR-PF estimates with large initial state mismatch and model error for VPO exhibiting stable limit cycle.

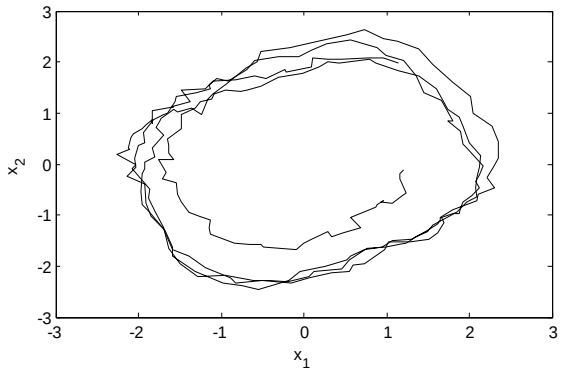

Fig. 6. Phase portrait of UPF estimates with large initial state mismatch and model error for VPO exhibiting stable limit cycle.

Case 3: Initial state mismatch and large measurement noise

The filter responses under the assumption of initial state mismatch and large measurement noise are discussed here. The parameter μ for both the system and the state estimator model is chosen as 0.4. The initial state is chosen as $x_0 = \begin{bmatrix} 1.2 & 0 \end{bmatrix}^{\mathrm{T}}$. The initial state estimate $(\hat{x}_0)$, initial state covariance (P), process noise covariance (Q) and measurement noise covariance (R) are chosen as

$$\hat{x}_0 = \begin{bmatrix} 0 & 3 \end{bmatrix}^{\mathrm{T}},$$

$$P_0 = \begin{bmatrix} 2 & 0 \\ 0 & 2 \end{bmatrix}, \quad Q = (0.05)^2 \begin{bmatrix} 1 & 0 \\ 0 & 1 \end{bmatrix} \quad \text{and}$$

$$R = (0.3)^2 \begin{bmatrix} 1 & 0 \\ 0 & 1 \end{bmatrix} \tag{35}$$

It is reasonable to assume higher value of measurement noise covariance for both the filters as this case deals with large measurement noise. The interesting finding from Fig. 7 is that in spite of considering large measurement noise and initial state vector mismatch, the UPF estimates converge to the true states and follow its trajectory, whereas the SIR-PF estimates could not converge to the true states as the estimates are obtained at each time instant without any knowledge of the measurements.The phase portrait of SIR-PF and UPF estimates subjected to large measurement noise covariance are shown in Figs. 8 and 9 respectively. The average RMSE values obtained for this condition are listed in third row of Table 1.

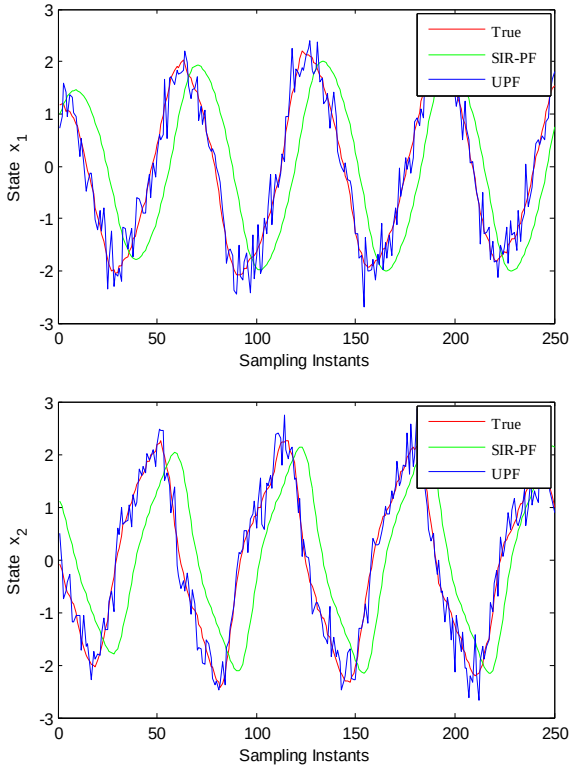

Fig. 7. Evolution of true and estimated states of VPO in forward time using SIR-PF and UPF with large initial state mismatch and measurement noise.

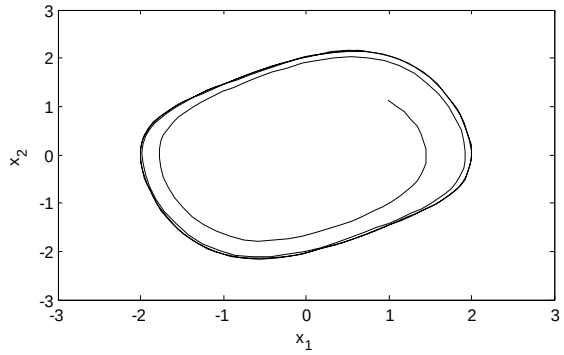

Fig. 8. Phase portrait of SIR-PF estimates with large initial state mismatch and measurement noise for VPO exhibiting stable limit cycle.

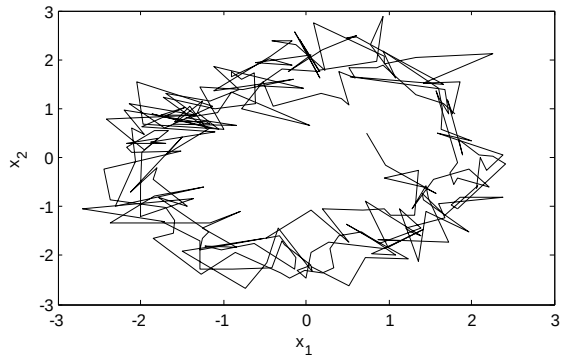

Fig. 9. Phase portrait of UPF estimates with large initial state mismatch and measurement noise for VPO exhibiting stable limit cycle.

5.3 State estimation of VPO under unstable limit cycle using particle filters

The unstable limit cycle of the VPO system has the property that all trajectories starting from points arbitrarily close to the limit cycle tend away from it as $t \to \infty$. In the case of an unstable limit cycle, if the initial state is inside the limit cycle, it converges to zero as time progresses. But instead, if the initial state is outside the limit cycle, it diverges.

Initially, the simulation study has been carried out to understand the behaviour of VPO system exhibiting unstable limit cycle in the absence of process and measurement noise. First, let us consider the initial state as $x_0 = \begin{bmatrix} 0.7 & 0 \end{bmatrix}^T$ which is well inside the limit cycle and $\mu = -0.3$. Fig. 10 shows that both the states of the system converge to zero as time progresses for the above assumed initial state. The phase portrait of the system under states converging condition is shown in Fig. 11.

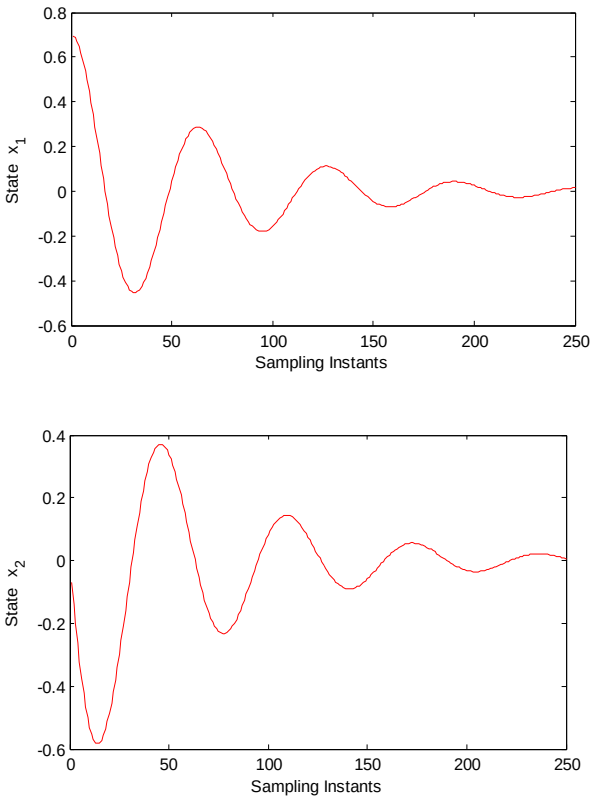

Fig. 10. Response of VPO in reverse time with an initial state inside the limit cycle.

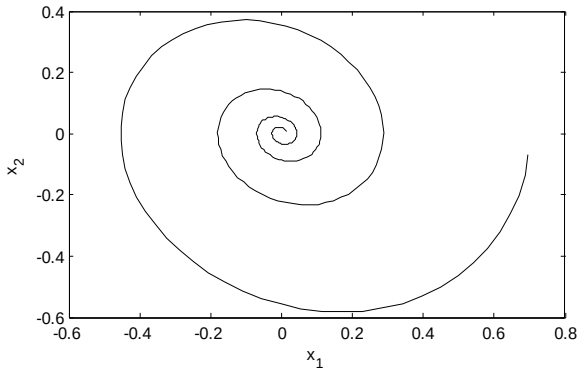

Fig. 11. Phase portrait of VPO exhibiting unstable limit cycle with an initial state inside the limit cycle.

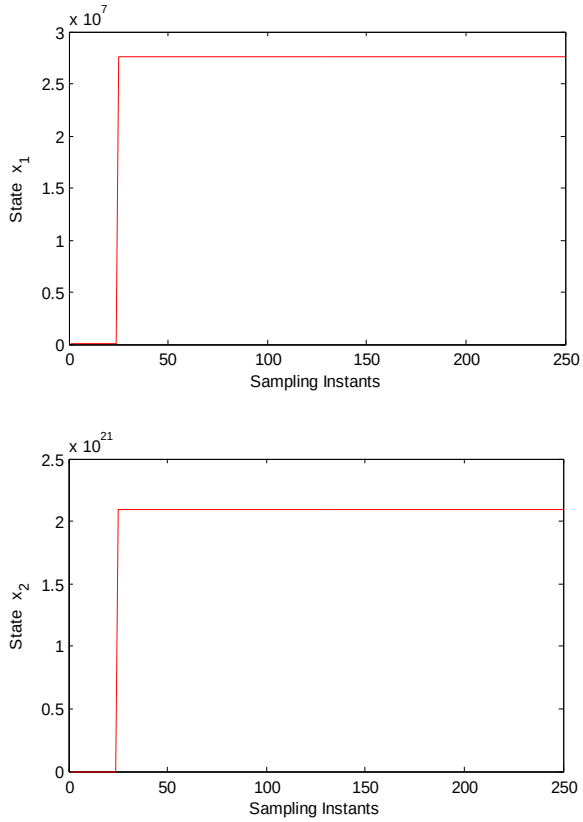

Fig. 12. Response of VPO in reverse time with an initial state outside the limit cycle.

On the other hand, consider the initial state as $x_0 = \begin{bmatrix} 0 & 2.5 \end{bmatrix}^T$ which is outside the limit cycle and the parameter $\mu = -0.3$. It can be observed in Fig. 12 that the states of the system diverge for the above assumed initial state and the phase portrait of the system under diverging conditions is shown in Fig. 13.

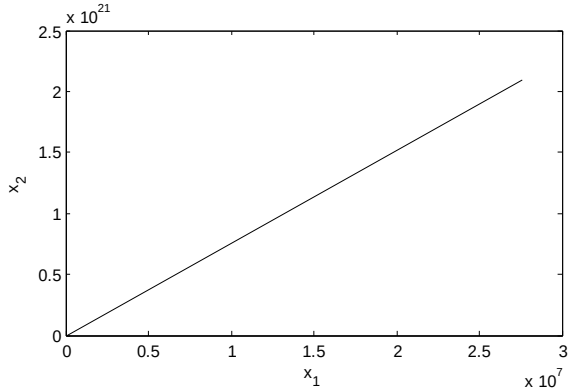

Fig. 13. Phase portrait of VPO exhibiting unstable limit cycle with an initial state outside the limit cycle.

The state estimation performance of UPF and SIR-PF for a VPO system with unstable limit cycle in the presence of stochastic process and measurement noise are analysed below for different conditions.

Case 1: Normal system operating conditions

The states of the system are estimated in this case without the initial state vector mismatch and model error. The value of the parameter μ is chosen as -0.3. The initial state (x_0) and the initial state estimate $(\hat{x}_0)$ are chosen as $\begin{bmatrix}0.7 & 0\end{bmatrix}^{\mathrm{T}}$ which is inside the limit cycle. The initial state covariance (P), process noise covariance (Q) and measurement noise covariance (R) are chosen as

$$P_0 = 10^{-2}\begin{bmatrix}1 & 0\\ 0 & 1\end{bmatrix},\quad Q = (0.05)^2\begin{bmatrix}1 & 0\\ 0 & 1\end{bmatrix} \quad \text{and}$$

$$R = (0.05)^2\begin{bmatrix}1 & 0\\ 0 & 1\end{bmatrix} \tag{36}$$

It is inferred from Fig. 14 that the UPF estimates captures the trajectory of the true states more closely than the SIR-PF estimates which does not converge to the true state as time progresses.

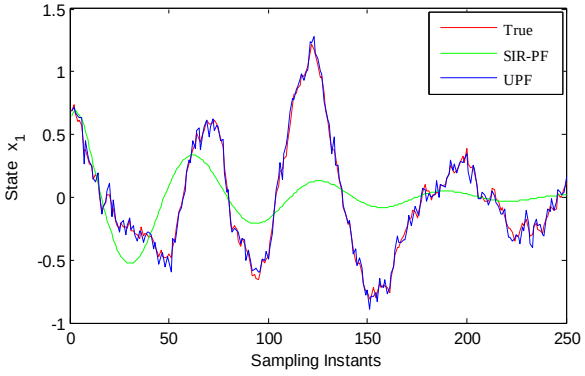

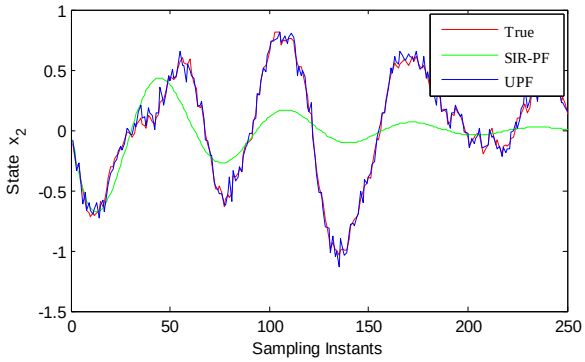

Fig. 14. Estimation performance of SIR-PF and UPF with an initial state estimate inside the limit cycle for VPO in reverse time.

Case 2: Initial state and model parameter mismatch

In the second case, the parameter μ for the system and the state estimator model is chosen as -0.3 and -0.5 respectively and thereby, introducing model parameter mismatch. The initial state is chosen as $x_0 = \begin{bmatrix}0.7 & 0\end{bmatrix}^{\mathrm{T}}$ which is inside the limit cycle. The initial state estimate is chosen as $\hat{x}_0 = \begin{bmatrix}0 & 2.5\end{bmatrix}^{\mathrm{T}}$ which is outside the limit cycle.

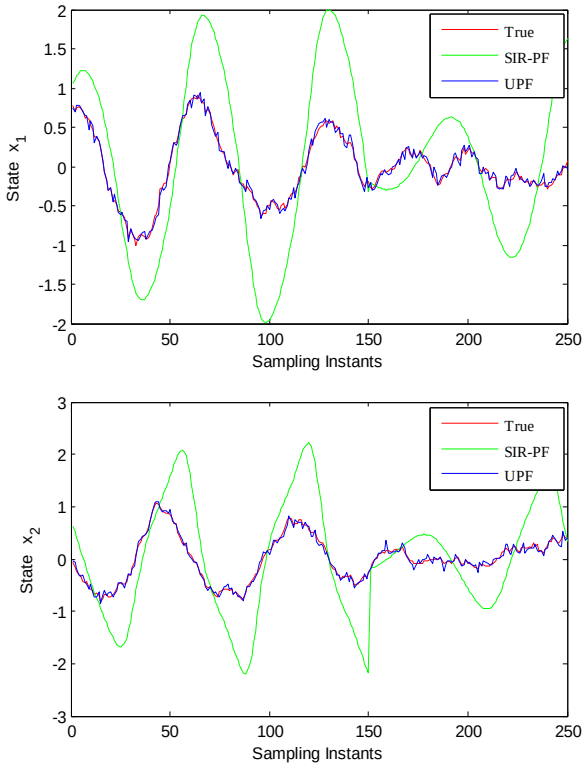

Fig. 15. Estimation performance of SIR-PF and UPF with an initial state estimate far from the limit cycle and with model error for VPO in reverse time.

The initial state covariance (P), process noise covariance (Q) and measurement noise covariance (R) are chosen as

$$P_0 = \begin{bmatrix} 1 & 0 \\ 0 & 1 \end{bmatrix}, \quad Q = (0.05)^2 \begin{bmatrix} 1 & 0 \\ 0 & 1 \end{bmatrix} \quad \text{and}$$

$$R = (0.05)^2 \begin{bmatrix} 1 & 0 \\ 0 & 1 \end{bmatrix} \tag{37}$$

Fig. 15 illustrates that the UPF attains the superior estimation results than the SIR-PF which results in large estimation error. It is also clear from Fig. 15 that the SIR filter estimates are more sensitive to the model error but the UPF provides higher degree of robustness to the model error. It is also noted that under high initial state mismatch, the UPF estimates converge at a faster rate as its state covariance decreases faster.

Case 3: Initial state mismatch and large measurement noise

It is assumed under this condition that for the system and estimator model, the value of μ is chosen as -0.3. The initial state is chosen as $x_0 = [0.7 \quad 0]^T$ which is inside the limit cycle. The initial state estimate is chosen as $\hat{x}_0 = [0 \quad 2.5]^T$ which is outside the limit cycle.

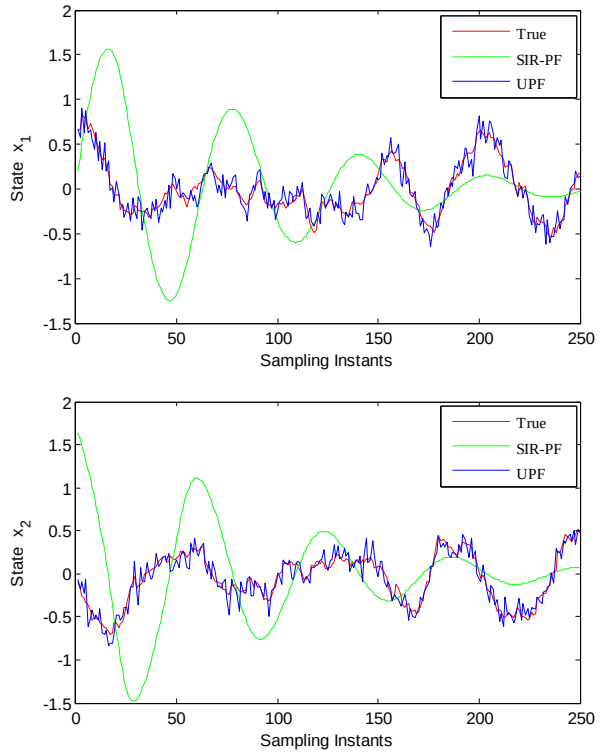

Fig. 16. Estimation performance of SIR-PF and UPF with an initial state estimate far from the limit cycle and with large measurement noise for VPO in reverse time.

The initial state covariance (P), process noise covariance (Q) and measurement noise covariance (R) are chosen as

$$P_0 = \begin{bmatrix} 1 & 0 \\ 0 & 1 \end{bmatrix}, \quad Q = (0.05)^2 \begin{bmatrix} 1 & 0 \\ 0 & 1 \end{bmatrix} \quad \text{and}$$

$$R = (0.2)^2 \begin{bmatrix} 1 & 0 \\ 0 & 1 \end{bmatrix} \tag{38}$$

It is observed from Fig. 16 that the UPF is much better in handling both initial state mismatch and large measurement noise and hence, achieves better state estimates than the SIR-PF. It also shows that the SIR filter is unable to track the true state as its particles are not able to lie in the region of the true state.

Table 2
State estimation performance of filter under different conditions for VPO exhibiting unstable limit cycle

Conditions	Average RMSE			
	SIR-PF Estimates		UPF Estimates	
	$\hat{x}_1$	$\hat{x}_2$	$\hat{x}_1$	$\hat{x}_2$
Normal system operating conditions	0.3701	0.3594	0.0471	0.0475
Initial state mismatch and model error	0.7776	0.8006	0.0481	0.0530
Initial state mismatch and large measurement noise	0.5619	0.5854	0.1018	0.0963

The average RMSE values of the UPF and SIR-PF estimates under the above three conditions for VPO system exhibiting unstable limit cycle are listed in Table 2 to assess the estimation performance.

6. Conclusion

This paper has demonstrated the effectiveness of the UPF for estimating the states of a highly nonlinear Van der Pol oscillator (VPO) and the results are compared with the SIR-PF. It is found through simulation studies that the UKF is better suited as proposal density in the particle filter because it incorporates the latest measurements before the evaluation of importance

weights. Hence, this UKF proposal allows the particles to move towards the high likelihood region. Even though the UKF which assumes Gaussian distribution is used for generating the proposal, the UPF serves to bring the particles closer to the true state and retains its ability to estimate non-Gaussian state distributions.

From the results, it can be inferred that the UPF outperforms the SIR-PF under normal system operating conditions, high initial state mismatch and large measurement noise. The UPF proves to be more robust to the error induced in the state estimator model of VPO. The filter performances are also evaluated for this nonlinear oscillator by calculating the RMSE values under different operating conditions. Hence, it is found that UPF can be the good choice for VPO because of its ability to provide more accurate estimation of states.

References

1. R. S. Barbosa, J. A. T. Machado, B. M. Vinagre, and A. J. Calderon, "*Analysis of the Van der Pol oscillator containing derivatives of fractional order*," J. Vib. Control, Vol. 13, No. 9-10, pp. 1291-1301, Sep. 2007.
2. R. Kandepu, B. Foss, and L. Imsland, "Applying the unscented Kalman filter for nonlinear state estimation," J. Process Contr., Vol. 18, No. 7-8, pp. 753-768, Aug. 2008.
3. R. Sajeeb, C. S. Manohar, and D. Roy, "*A semi-analytical particle filter for identification of nonlinear oscillators*," Probabilist. Eng. Mech., Vol. 25, No. 1, pp. 35-48, Jan. 2010.
4. H. K. Khalil, *Nonlinear Systems*, Prentice Hall, pp. 41-47, 2000.
5. I. M. Ginarsa, A. Soeprijanto, and M. H. Purnomo, "*Controlling chaos and voltage collapse using an ANFIS-based composite controller-static var compensator in power systems*," Int. J. Elec. Power, Vol. 46, pp. 79-88, March 2013.
6. R. E. Precup, M. L. Tomescu, and C. A. Dragos, "*Stabilization of Rossler chaotic dynamical system using fuzzy logic control algorithm*," Int. J. Gen. Syst., Vol. 43, No. 5, pp. 413-433, Feb. 2014.
7. S. K. Choudhary, "*LQR based optimal control of chaotic dynamical systems*," Int. J. Model. Simul., Vol. 35, No. 3-4, pp. 104-112, Dec. 2015.
8. A. Bouzeriba, A. Boulkroune, and T. Bouden, "*Projective synchronization of two different fractional-order chaotic systems via adaptive fuzzy control*," Neural Comput. Appl., Vol. 27, No. 5, pp. 1349-1360, July 2016.
9. M. Barurt, S. Bogosyan, and M. Gikasan, "Speed-sensorless estimation for induction motors using extended Kalman filter," IEEE Trans. Ind. Electron., Vol. 54, No. 1, pp. 272-280, Feb. 2007.
10. S. Kumar, J. Prakash, and P. Kanagasabapathy, "*A critical evaluation and experimental verification of extended Kalman filter, unscented Kalman filter and neural state filter for state estimation of three phase induction motor*," Appl. Soft Comput., Vol. 11, No. 3, pp. 3199-3208, April 2011.
11. P. Terwiesch and M. Agarwal, "*A discretized nonlinear state estimator for batch processes*," Comput. Chem. Eng., Vol. 19, No. 2, pp. 155-169, Feb. 1995.
12. R. E. Kalman, "*A new approach to linear filtering and prediction problems*," J. Basic Eng.-T ASME, Vol. 82, No. 1, pp. 35-45, 1960.
13. A. H. Jazwinski, *Stochastic Process and Filtering Theory*, Academic Press, pp. 142-158, 1970.
14. A. Gelb, *Applied Optimal Estimation*, M.I.T. Press, pp. 102-107, 1974.
15. E. A. Wan and R. Van der Merwe, "*The unscented Kalman filter for nonlinear estimation*," in Proceedings of IEEE Symposium (AS-SPCC), Lake Louise, Alberta, Canada, pp. 153-158, 2000.
16. S. J. Julier and J. K. Uhlmann, "*Unscented filtering and nonlinear estimation*," in Proceedings of IEEE, Vol. 92, No. 3, pp. 401-422, March 2004.
17. N. Gordon, D. Salmond, and A. F. M. Smith, "*Novel approach to nonlinear and non-Gaussian Bayesian state estimation*," IEE Proc.-F, Vol. 140, No. 2, pp. 107-113, 1993.
18. T. Chen, J. Morris, and E. Martin, "*Particle filtering for state and parameter estimation in batch processes*," J. Process Contr., Vol. 15, No. 6, pp. 665-673, Sep. 2005.
19. R. Van der Merwe, A. Doucet, N. de Freitas and E. Wan, *The Unscented Particle Filter*, Tech. Rep. CUED/F-INFENG/TR 380, Department of Engineering, University of Cambridge, UK, 2000.
20. X. Ning and J. Fang, "*Spacecraft autonomous navigation using unscented particle filter–based celestial/doppler information fusion*," Meas. Sci. Technol., Vol. 19, No. 9, pp. 1-8, 2008.
21. A. V. Shenoy, J. Prakash, K. B. McAuley, V. Prasad V, and S. L. Shah, "*Practical issues in the application of the particle filter for estimation of chemical processes*," in Proceedings of 18th IFAC World Congress, Milano, Italy, pp. 2773-2778, 2011.
22. Y. Shen, "*Hybrid unscented particle filter based state-of-charge determination for lead-acid batteries*," Energy, Vol. 74, No.1, pp. 795-803, 2014.
23. G. G. Rigatos, "*Particle filtering for state estimation in nonlinear industrial systems*," IEEE Trans. Instrum. Meas., Vol. 58, No. 11, pp. 3885-3900, Nov. 2009.
24. O. Aydogmus and M. F. Talu, "*Comparison of Extended-Kalman-and particle-filter-based sensorless speed control*," IEEE Trans. Instrum. Meas., Vol. 61, No. 2, pp. 402-410, Feb. 2012.
25. J. W. Lee, Y. S. T. Hong, C. Suh, and H. S. Shin, "*Online nonlinear sequential Bayesian estimation of a biological wastewater treatment process*," Bioproc. Biosyst. Eng., Vol. 35, No. 3, pp. 359-369, July 2012.
26. F. Kwasniok, "*Estimation of noise parameters in dynamical system identification with Kalman filters*,"

Phys. Rev. E, Vol. 86, pp. 1-8, 2012.
27. I. Dumitrescu, S. Bachir, D. Cordeau, J. M. Paillot, and M. Lordache, "*Modeling and characterization of oscillator circuits by Van der Pol model using parameter estimation*," J. Circuit. Syst. Comp., Vol. 21, No. 5, pp. 1-15, 2012.
28. M. Arulampalam, S. Maskell, N. Gordon, and T. Clapp, "*A tutorial on particle filters for online nonlinear/Non-Gaussian Bayesian tracking*," IEEE Trans. Signal Process., Vol. 50, No. 2, pp. 174-188, 2002.
29. B. Ristic, S. Arulampalam, and N. Gordon, *Beyond the Kalman Filter: Particle Filters for Tracking Applications*, Artech House, pp. 35-57, 2004.
30. A. Romanenko and J. A. A. M. Castro, "*The unscented filter as an alternative to the EKF for nonlinear state estimation: A simulation case study*," Comput. Chem. Eng., Vol. 28, No. 3, pp. 347-355, March 2004.
31. G. G. Rigatos, "*Particle and Kalman filtering for state estimation and control of DC motors*," ISA Trans., Vol. 48, No. 1, pp. 62-72, Jan. 2009.